

COUNTING PLANAR DIAGRAMS WITH VARIOUS RESTRICTIONS

Gerard 't Hooft

Institute for Theoretical Physics
University of Utrecht, Princetonplein 5
3584 CC Utrecht, the Netherlands
e-mail: g.thoof@phys.uu.nl

Abstract

Explicit expressions are considered for the generating functions concerning the number of planar diagrams with given numbers of 3- and 4-point vertices. It is observed that planar renormalization theory requires diagrams with restrictions, in the sense that one wishes to omit ‘tadpole’ inserions and ‘seagull’ insertions; at a later stage also self-energy insertions are to be removed, and finally also the dressed 3-point inserions and the dressed 4-point insertions. Diagrams with such restrictions can all be counted exactly. This results in various critical lines in the λ - g plane, where λ and g are effective zero-dimensional coupling constants. These lines can be localized exactly.

1. Introduction

In Quantum Chromodynamics (QCD), with N color degrees of freedom and gauge coupling constant g , the limit $N \rightarrow \infty$ and $g \rightarrow 0$, such that $N g^2 = \tilde{g}^2$ is kept fixed, leads to a \tilde{g} expansion, for which all feynman diagrams are planar¹. The $1/N$ expansion, at higher orders in N , requires diagrams on planes with non-trivial topology.

In this paper, we only consider the \tilde{g} expansion at infinite N . If \tilde{g} is sufficiently large, this expansion diverges. Since the theory is asymptotically free, \tilde{g} is small in the

ultraviolet region, so that, there, small diagrams dominate. An important question is, how the infrared region is affected by the fact that the \tilde{g} expansion has a finite region of convergence. Naively, one might expect an infrared Landau ghost, but it is more likely that a delicate rearrangement mechanism will take place that will strongly affect the physical spectrum of states. One might conjecture that this rearrangement mechanism may cause quark confinement in the $N \rightarrow \infty$ limit.ref2

To this end, we study the critical effects for large \tilde{g} 's in a zero-dimensional model. The 'field theory' is described by the action

$$S(M) = \text{Tr} \left(-\frac{1}{2}M^2 + \frac{1}{3}gM^3 + \frac{1}{4}\lambda M^4 \right), \quad (1.1)$$

where M is an $N \times N$ dimensional matrix, in the limit

$$N \rightarrow \infty, \quad g, \lambda \rightarrow 0, \quad Ng^2 = \tilde{g}^2 \text{ and } N\lambda = \tilde{\lambda} \text{ fixed.} \quad (1.2)$$

Henceforth, the tilde ($\tilde{}$) will be omitted. The main body of the paper consists of the calculation of the generating functions for the number of planar diagrams with various types of restrictions on them. The motivation for the restrictions stems from a special renormalization program that is particularly suitable for planar QCD. This program is deferred to Appendix A, so as not to interrupt the most important theme of the paper.

We study many different cases, all related one to another by exact equations. It is important to have a consistent notation. Unfortunately, existing notations were too haphazard, so we had to invent our own. This is explained in Section 2.

Much of this paper is based on pioneering work by Koplik, Neveu and Nussinov³ – which in turn makes use of earlier work by Tutte⁴ – and on the work by Brézin, Itzykson, Parisi and Zuber⁵. The latter apply matrix theory to do the integration with the action (1.1). Here, we choose, instead, to work directly from the functional equations, as these will be easier to handle in the QCD case, and they are also more transparent in diagrammatic approaches. The relations are read off directly from the diagrams.

A delicate problem then is the choice of boundary conditions for these equations. They can be derived by carefully considering the holomorphic structure that the generating functions are required to have. Once this is understood, a fundamental solution is obtained for the generating function describing *the numbers of all planar diagrams for all multiparticle connected Green functions, with given numbers V_3 of three-point vertices, V_4 four-point vertices, and E external lines.* It is derived in Sect. 3. From this function, all other cases can be derived (Sections 4–8).

Combining the results, we find the regions in the g, λ plane where the planar diagram summations (over different kinds of planar diagrams),

$$\sum_{V_3, V_4} N_a(V_3, V_4, E) g^{V_3} \lambda^{V_4}, \quad (1.3)$$

converge. Here, N_a , $a = 0, 1, 2, \dots$ refers to the number of diagrams with different kinds of restrictions, labeled by the number a .

An accurate picture of the resulting regions is shown in Fig. 7. Conclusions are summed up in Sect. 10.

Many of our results were obtained and/or checked using the computer program *Mathematica*.

2. General notation

We define

$$\begin{aligned} V_3 &= \# \text{ 3-point vertices,} \\ V_4 &= \# \text{ 4-point vertices,} \\ E &= \# \text{ external lines.} \end{aligned} \tag{2.1}$$

For the generating function for the number of Green functions that *include the disconnected diagrams*, we use the symbol G :

$$G(\eta, g, \lambda) \equiv \sum_{\substack{E=0, \\ V_3=0, V_4=0}}^{\infty, \infty, \infty} \eta^E g^{V_3} \lambda^{V_4} G_{(E, V_3, V_4)} . \tag{2.2}$$

Most often, we shall concentrate on the generating functions for *connected diagrams* only. They will be denoted by the letter F :

$$F(z, g, \lambda) \equiv \sum_{\substack{E=1, \\ V_3=0, V_4=0}}^{\infty, \infty, \infty} z^{E-1} g^{V_3} \lambda^{V_4} F_{(E-1, V_3, V_4)} . \tag{2.3}$$

Here, it is for technical reasons that we start counting at $E = 1$, which will become clear. Note, also, that we use a different symbol z , instead of η . This is also for later convenience.

The *one-particle irreducible* (1PI) diagrams will be generated by the function Γ :

$$\Gamma(u, g, \lambda) \equiv \sum_{\substack{E=1, \\ V_3=0, V_4=0}}^{\infty, \infty, \infty} u^{E-1} g^{V_3} \lambda^{V_4} \Gamma_{(E-1, V_3, V_4)} . \tag{2.4}$$

Apart from limiting ourselves to connected or irreducible diagrams, we can also make restrictions on the occurrence of insertions within the (reducible or irreducible) regions of the diagrams. This we indicate by using a subscript a , taking values between 0 and 5, defined as in the following list. The symbols G , F , Γ , and the variables g, λ, η, z , and u , are all replaced, successively, by G_a , F_a , Γ_a , $g_a, \lambda_a, \eta_a, z_a$, and u_a , meaning:

$$a = 0, (G_0, F_0, \dots) : \text{ no further restrictions.} \tag{2.5}$$

$$a = 1, (G_1, F_1, \dots) : \text{ no tadpoles: } \text{---} \text{\textcircled{X}} \tag{2.6}$$

$$a = 2 : \quad \text{no tadpoles and no seagulls:} \quad \text{---} \circ \text{---} \quad (2.7)$$

$$a = 3 : \quad \text{also no self-energies:} \quad \text{---} \circ \text{---} \quad (2.8)$$

$$a = 4 : \quad \text{also no dressed 3-vertices:} \quad \text{---} \circ \text{---} \quad (2.9)$$

$$a = 5 : \quad \text{also no dressed 4-vertices:} \quad \text{---} \circ \text{---} \quad (2.10)$$

It will turn out to be important to use the subscripts also for the variables $g, \lambda, \eta, z,$ and u . The reader may appreciate that the use of these suffixes is to be preferred rather than exploiting the entire Latin and Greek alphabets. The price paid is slightly more complicated-looking expressions. Where ambiguities can be avoided, we will suppress some of the subscripts.

In Eq. (1.1), our action is defined. Notice, that, in contrast with usual conventions, we chose the signs in front of the interaction terms to be positive. Therefore, the positive values of the coupling constants are the unstable ones. The reason for this unorthodox choice is that now the expansions in terms of g_a and λ_a all carry plus signs. With this sign convention, the coefficients directly correspond to the number of diagrams. Furthermore, unlike Ref ⁵, we chose factors $1/3$ and $1/4$ in front of the coupling terms. This is quite conventional. In our case, these are the best combinatorial factors to choose. The coefficients of all expansion terms will be integers, and the only multiplicity factors with which diagrams are counted, are the ones corresponding to how many ways a diagram can be rotated into distinct forms. In Fig. 1, these multiplicity factors for some diagrams are indicated.

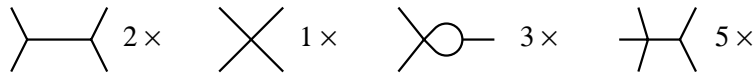


Figure 1.
Multiplicity factors for some diagrams.

3. The primary equations

The recursion equations are most easily derived for the generating function $F = F_0$ describing all connected planar diagrams. Diagrammatically, we have Fig. 2. Since, in this entire section, we will be limiting ourselves to the case $a = 0$ (no further restrictions), we temporarily omit the subscripts 0 that indicate this (so F, g, λ, \dots stand for $F_0, g_0, \lambda_0, \dots$).

Writing

$$F(z, g, \lambda) = F_{(0)}(g, \lambda) + z F_{(1)}(g, \lambda) + z^2 F_{(2)}(g, \lambda) + \dots \quad (3.1)$$

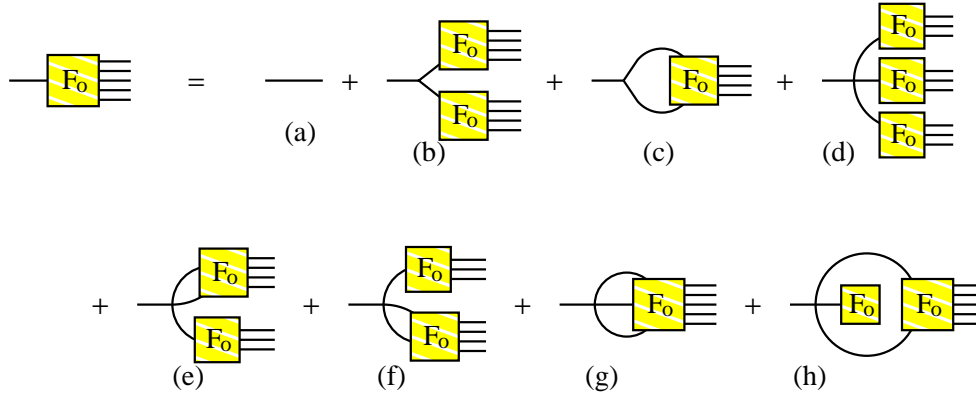


Figure 2. Equation (3.2)

(using brackets to distinguish the subscripts of the Taylor expansion from the subscript a), the equation of Fig. 2 reads:

$$\begin{aligned}
 F = z + g \left(F^2 + \frac{F - F_{(0)}}{z} \right) + \\
 \lambda \left(F^3 + 2F \frac{F - F_{(0)}}{z} + \frac{F - F_{(0)} - F_{(1)}z}{z^2} + F_{(0)} \frac{F - F_{(0)}}{z} \right). \tag{3.2}
 \end{aligned}$$

The last term is very important. If one does not take it into account, the resulting equations, at a later stage, lead to horrendous complications impeding explicit solution*

The contributions of $F_{(0)}$ and $F_{(1)}$ are necessary for removing unwanted contributions from Green functions with too few external lines to close the loops in diagrams (c) and (e)–(h) in Fig. 2.

Clearly, one can solve Eq. (3.2) if $F_{(0)}$ and $F_{(1)}$ are known. The trick to find these was described by Koplik et al³, and goes back to Tutte⁴. However, we need the result for general g and λ , and it appears to be difficult to extend their method directly. The matrix integration procedure used by Brézin et al⁵, for pure $g M^3$ and pure λM^4 theory, does work, also for our more general case, but we can easily reproduce this general result without integrating over matrices. What needs to be done, as Brézin et al did, is first to concentrate on the general Green functions G_0 , instead of the connected ones, F_0 .

The relation between G_a and F_a is simple to derive diagrammatically. Consider a (connected or disconnected) diagram G . Draw a circle around it, such that the circle is cut into E pieces by the E external lines. Select one of these E pieces as a starting point. This breaks the rotational symmetry, and consequently any diagram with E external lines will be counted E/S times, where S is the dimension of the rotational symmetry group of the diagram (cf Fig. 1). We open the circle at this point, and then find the relation between F and G diagrammatically. See Fig. 3. In this Figure, the wiggled line represents

* In principle, Eqs. of the form (3.16)–(3.21) can then still be derived, but they become expressions involving polynomials whose degrees are well over 100, containing coefficients that are integers with hundreds of decimal places.

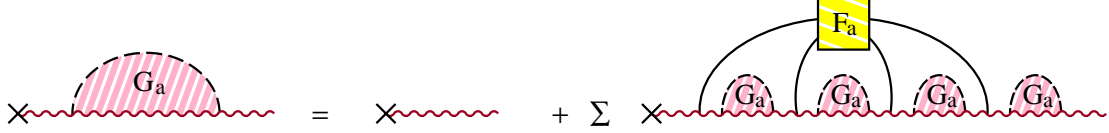


Figure 3. Recursive equation relating G_a and F_a

the circle that was opened up. The cross is the arbitrary point at the boundary that was selected.

The resulting equation, which turns out to hold for all $a = 0, \dots, 5$, is

$$G(\eta) = 1 + \sum_{E=1}^{\infty} F_{(E-1)}(g, \lambda) (G(\eta))^E \eta^E = 1 + \eta G(\eta) F(\eta G(\eta), g, \lambda). \quad (3.3)$$

Hence,

$$F(\eta G(\eta), g, \lambda) + \frac{1}{\eta G(\eta)} = \frac{1}{\eta}. \quad (3.4)$$

Noticing, that $\eta G(\eta)$ acts as z variable in the function F , we rewrite this equation by making the following identifications in Eqs. (2.2) and (2.3):

$$G_a = 1 + z_a F_a = \frac{z_a}{\eta_a}, \quad (3.5)$$

$$\frac{1}{\eta_a} = F_a + \frac{1}{z_a}. \quad (3.6)$$

(valid for all $a = 0, \dots, 5$).

Substituting (3.6) into (3.2) gives us the recursive equation for $G(\eta)$:

$$z + \left(x - \frac{1}{z}\right)(-1 + gx + \lambda x^2) - \frac{1}{z}(\alpha x + \beta) = 0, \quad (3.7)$$

where

$$x = \frac{1}{\eta} = F + \frac{1}{z}; \quad (3.8)$$

$$\alpha(g, \lambda) = \lambda F_{0(0)}; \quad \beta(g, \lambda) = g F_{0(0)} + \lambda F_{0(1)} + \lambda F_{0(0)}^2; \quad (3.9)$$

$$z = \eta G(\eta), \quad (3.10)$$

and all this only holds for $a = 0$. The symbol x is the same as the one used to describe the Eigenvalues of the matrices M , by Brézin et al ⁵.

As this equation is only quadratic[†] in z , it is easy to solve:

$$2z = x - gx^2 - \lambda x^3 \pm \sqrt{x^2(1 - gx - \lambda x^2)^2 + 4(\lambda x^2 + (g - \alpha)x + \beta - 1)}. \quad (3.11)$$

[†] Here, the last term of Eq. (3.2), diagram (h) in Fig. 2, was crucial.

The, as yet unknown, functions $\alpha(g, \lambda)$ and $\beta(g, \lambda)$ can now be determined by repeating the arguments by Tutte⁴ and Koplik et al³, and Brézin et al⁵. We contemplate the branch points by looking at the roots of the 6th degree polynomial in x under the square root symbol, as λ, g, α and β become small. At x small compared to $1/g$ and $1/\sqrt{\lambda}$ (which means η large compared to g and $\sqrt{\lambda}$), there are only two roots,

$$x = x_{1,2} \approx \pm 2 + \mathcal{O}(g, \sqrt{\lambda}). \quad (3.12)$$

All other roots must be at much larger values of x , i.e. $\eta = \mathcal{O}(g, \sqrt{\lambda})$. Branch points at such small values of η are inadmissible, however, and therefore they must cancel out pairwise. Thus, for the other roots, one must demand

$$x_3 = x_4 ; \quad x_5 = x_6 . \quad (3.13)$$

This means that it must be possible to write Eq. (3.11) as

$$2z = x - gx^2 - \lambda x^3 \pm \lambda(x - x_3)(x - x_5)\sqrt{(x - x_1)(x - x_2)}. \quad (3.14)$$

It can also be seen from Eq. (3.5) that, for large x , the function z , with the appropriate sign choice for the square root, goes as $1/x$, but we do not need this information here.

In order to bring the ensuing expressions into a slightly simpler form, we rewrite

$$x_1 + x_2 = 2p ; \quad x_1 x_2 = -4 + p^2 - 4q . \quad (3.15)$$

In view of Eq. (3.12), this implies that p and q will be of order g and λ . The requirement that Eq. (3.11) can be written in the form (3.14), because of Eqs. (3.13), implies two constraints, which fix the functions $\alpha(g, \lambda)$ and $\beta(g, \lambda)$. Explicitly, what one finds is:

$$g = \frac{p(3 + 3p^2 - 3q^2 + 2p^2q)}{(1+q)(6 - 3p^2 + p^4 + 12q - 3p^2q + 6q^2)} ; \quad (3.16)$$

$$\lambda = \frac{2q - 2p^2 + 2q^2 - p^2q}{(1+q)(6 - 3p^2 + p^4 + 12q - 3p^2q + 6q^2)} ; \quad (3.17)$$

$$\alpha = \frac{p(2q - 2p^2 + 2q^2 - p^2q)(3 + p^4 + 3q + p^2q - 3q^2 + p^2q^2 - 3q^3)}{(1+q)(6 - 3p^2 + p^4 + 12q - 3p^2q + 6q^2)^2} ; \quad (3.18)$$

$$\beta = \frac{\left(12q - 3p^2 + 11p^4 - 5p^6 + p^8 - 28p^2q + 30p^4q - 6p^6q + \right. \\ \left. + 32q^2 - 46p^2q^2 + 19p^4q^2 + 24q^3 - 20p^2q^3 + p^2q^4 - 4q^5 \right)}{(6 - 3p^2 + p^4 + 12q - 3p^2q + 6q^2)^2} , \quad (3.19)$$

and with Eqs. (3.9):

$$A \equiv F_{0(0)} = \frac{p(3 + p^4 + 3q + p^2q - 3q^2 + p^2q^2 - 3q^3)}{6 - 3p^2 + p^4 + 12q - 3p^2q + 6q^2} ; \quad (3.20)$$

$$B \equiv F_{0(1)} = \frac{(1+q) \begin{pmatrix} 36 - 33p^2 + 33p^4 - 13p^6 + p^8 + 132q - 105p^2q \\ + 85p^4q - 18p^6q + 168q^2 - 126p^2q^2 + 77p^4q^2 \\ - 6p^6q^2 + 72q^3 - 78p^2q^3 + 31p^4q^3 - p^6q^3 \\ - 12q^4 - 33p^2q^4 + 6p^4q^4 - 12q^5 - 9p^2q^5 \end{pmatrix}}{(6 - 3p^2 + p^4 + 12q - 3p^2q + 6q^2)^2} . \quad (3.21)$$

The way to interpret these equations is that p and q should be eliminated, to find A and B as functions of g and λ .

The elimination process induces singularities as branch points in the 4-dimensional space of complex g, λ values. These in turn determine the convergence of the combined (g, λ) expansion. Since all expansion parameters for $F_{0(0)}$ and $F_{0(1)}$ must be non-negative integers, the singularities at real and positive values for g and λ are of particular relevance. They will further be discussed in Section 9 and Appendix C.

Two special cases are:

1) $g\phi^3$ theory:

$$\lambda = 0 ; \quad p^2 = \frac{2q(1+q)}{2+q} . \quad (3.22)$$

In this case, direct solution[‡] leads to a single parameter, $\sigma = g/p$, replacing p and q :

$$p^2 = \frac{2\sigma}{(1-\sigma)(1-2\sigma)} ; \quad q = \frac{2\sigma}{1-2\sigma} ; \quad \alpha = 0 ; \quad (3.23)$$

$$g^2 = \frac{\sigma^2}{p^2} = \frac{1}{2}\sigma(1-\sigma)(1-2\sigma) ; \quad (3.24)$$

$$\beta = g F_{0(0)} = \frac{\sigma(1-3\sigma)}{2(1-2\sigma)} . \quad (3.25)$$

The last two equations determine the function $F_{0(0)}(g)$, which is here the only function needed to solve Eq. (3.2).

2) $\lambda\phi^4$ theory:

$$g = 0 ; \quad p = 0 ; \quad \alpha = 0 ; \quad (3.26)$$

$$\lambda = \frac{q}{3(1+q)^2} ; \quad F_{0(0)} = 0 ; \quad (3.27)$$

$$\beta = \lambda F_{0(1)} = \frac{q(3-q)}{9(1+q)} . \quad (3.28)$$

[‡] Different procedures lead to different auxiliary parameters^{3,4,5}, but these can all be related one to another by one-to-one mappings. Up to a sign, the parameter σ shown here is the one used by Brézin et al⁵.

4. One-particle-irreducible diagrams

The generating function Γ for one-particle-irreducible (1PI) diagrams has been treated in Ref³. Here, we briefly review the procedure. The treatments of this Section hold for all cases $a = 0, \dots, 5$, so we suppress the suffix a .

Let

$$\begin{aligned} \Gamma(u) &= -u + g u^2 + \lambda u^3 + \text{loop corrections} \\ &= -u + \Gamma_{(0)} + \tilde{\Gamma}_{(1)} u + \Gamma_{(2)} u^2 + \dots, \end{aligned} \quad (4.1)$$

where $\tilde{\Gamma}_{(1)} = \Gamma_{(1)} + 1$ denotes the self-energy contributions containing at least one vertex. The relation between Γ and F can be seen diagrammatically, see Fig. 4.

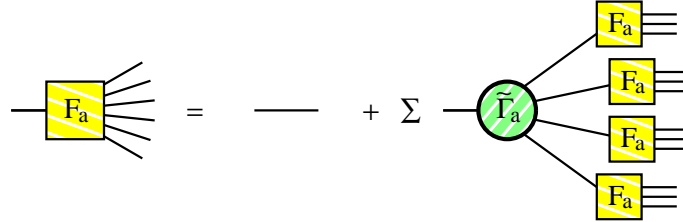


Figure 4. Equation (4.2) for Γ

This Figure corresponds to the equation

$$F(z) = z + \Gamma_{(0)} + \tilde{\Gamma}_{(1)} F(z) + \Gamma_{(2)} (F(z))^2 + \dots, \quad (4.2)$$

or:

$$-z = \Gamma(F(z)). \quad (4.3)$$

We write

$$\Gamma_a = -z_a = -\eta_a G_a; \quad (4.4)$$

$$u_a = F_a = \frac{1}{\eta_a} - \frac{1}{z_a} = \frac{G_a - 1}{z_a}. \quad (4.5)$$

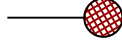
For a small number of external lines, and if $F_{(0)}$ and $\Gamma_{(0)}$ vanish, the relations between the coefficients $\Gamma_{(i)}$ and $F_{(i)}$ are straightforward:

$$-z = \Gamma_{(1)}(F_{(1)}z + F_{(2)}z^2 + F_{(3)}z^3 \dots) + \Gamma_{(2)}(F_{(1)}z + F_{(2)}z^2 \dots)^2 + \Gamma_{(3)}(F_{(1)}z \dots)^3 + \dots, \quad (4.6)$$

or

$$\begin{aligned} \Gamma_{(1)} &= -\frac{1}{F_{(1)}}; & \Gamma_{(2)} &= \frac{F_{(2)}}{F_{(1)}^2}; & \Gamma_{(3)} &= \frac{F_{(1)}F_{(3)} - 2F_{(2)}^2}{F_{(1)}^5}; \\ \Gamma_{(4)} &= \frac{1}{F_{(1)}^7} [F_{(1)}^2 F_{(4)} + 5F_{(2)}^3 - 5F_{(1)}F_{(2)}F_{(3)}], & & \text{etc.} \end{aligned} \quad (4.7)$$

5. Removing tadpole insertions ($a = 1$)



Vacuum expectation values of single field operators often vanish. In QCD, global gauge-invariance is sufficient to see that

$$\langle 0 | A_{\mu_j}^i(x) | 0 \rangle = 0. \quad (5.1)$$

In our case, this amplitude is $F(0, g, \lambda) = F_{0(0)}$. We now concentrate on the case $a = 1$, where we impose that all contributions of this sort are omitted. Clearly, the last diagram (h) of Fig. 2 is now absent. But also diagrams (c) and (g) require modifications, as they might produce the unwanted tadpole contributions. We thus obtain

$$F_{1(0)} = 0, \quad (5.2)$$

and removing all contributions to $F_{1(0)}$, we see that Eq. (3.2) is replaced by

$$\begin{aligned} F(z, g, \lambda) = & z + g \left(F^2 + \frac{F - F_{(1)}z}{z} \right) + \\ & + \lambda \left(F^3 + \frac{2F^2}{z} + \frac{F - F_{(1)}z - F_{(2)}z^2}{z^2} \right), \quad \text{if } a = 1. \end{aligned} \quad (5.3)$$

Here, F, z, g, λ, \dots all stand for $F_1, z_1, g_1, \lambda_1, \dots$

There are two ways to proceed with this equation. First, one can again write $x_1 = F_1 + 1/z_1$, to obtain a quadratic equation for z_1 as a function of x_1 :

$$z_1 + \left(x_1 - \frac{1}{z_1} \right) (\lambda_1 x_1^2 + g_1 x_1 - 1) - (g_1 F_{1(1)} + \lambda_1 F_{1(2)}) - \frac{\lambda_1 F_{1(1)}}{z_1}, \quad (5.4)$$

and we can proceed as in Sect. 3.

It is instructive, however, to find the direct relations between F_1, z_1, g_1, \dots on the one hand, and F_0, z_0, g_0, \dots on the other:

$$F_1 = Q_1(F_0 - F_{0(0)}); \quad (5.5)$$

$$z_1 = \frac{z_0}{Q_1}, \quad \text{hence} \quad x_1 = Q_1(x_0 - F_{0(0)}); \quad (5.6)$$

$$g_1 = \frac{g_0 + 3\lambda_0 F_{0(0)}}{Q_1^3}; \quad \lambda_1 = \frac{\lambda_0}{Q_1^4}. \quad (5.7)$$

The form of the function $Q_1(g, \lambda)$ can be read off from the requirement that, after the transformation, the Lagrangian again has a kinetic part normalized to one:

$$\mathcal{L} = -\frac{1}{2}x_0^2 - \frac{1}{3}g_0x_0^3 - \frac{1}{4}\lambda_0x_0^4 = C + Dx_1 - \frac{1}{2}x_1^2 - \frac{1}{3}g_1x_1^3 - \frac{1}{4}\lambda_1x_1^4, \quad (5.8)$$

from which one reads off Eqs. (5.5)–(5.7), and

$$Q_1^2 = 1 - 2g_0 F_{0(0)} - 3\lambda_0 F_{0(0)}^2 . \quad (5.9)$$

The coefficient D is adjusted so as to obey Eq. (5.2), and the constant C is irrelevant.

Indeed, one checks that with the substitutions (5.5)–(5.7) and (5.9), the Eq. (3.2) turns into Eq. (5.3). In practice, this is the safe method: to adjust the transformations in such a way that the new recursion equation holds.

Since the coupling constants g_1 and λ_1 are now new functions of p and q , their critical values will also be displaced. The fact that the critical values also follow the transformation rules (5.5)–(5.7) is not quite self-evident. But it is true, and related to the general feature that $dF_{0(0)}$ and $dF_{0(1)}$ vanish as soon as dp and dq are such that dg_0 and $d\lambda_0$ vanish. We return to this issue in Sect. 9.

6. Removing seagull insertions ($a = 2$)



The recursion relation for diagrams where tadpole and seagull insertions are removed, reads:

$$\begin{aligned} F(z, g, \lambda) = & z + g \left(F^2 + \frac{F - F_{(1)}z}{z} \right) + \\ & + \lambda \left(F^3 + 2F \frac{F - F_{(1)}z}{z} + \frac{F - F_{(1)}z - F_{(2)}z^2}{z^2} \right) , \end{aligned} \quad (6.1)$$

where now $F, z, g, \lambda \dots$ stand for $F_2, z_2, g_2, \lambda_2, \dots$

As the seagulls only affect the dressed propagators, the relation between F_2 and F_0 is as in Eqs. (5.5)–(5.7), but with a different choice for Q . We find that Eq. (6.1) is obeyed provided that

$$F_2 = Q_2(F_0 - F_{0(0)}) ; \quad (6.2)$$

$$z_2 = \frac{z_0}{Q_2} , \quad \text{so} \quad x_2 = Q_2(x_0 - F_{0(0)}) ; \quad (6.3)$$

$$g_2 = \frac{g_0 + 3\lambda_0 F_{0(0)}}{Q_2^3} ; \quad \lambda_1 = \frac{\lambda_0}{Q_2^4} ; \quad (6.4)$$

$$Q_2^2 = 1 - 2g_0 F_{0(0)} - 3\lambda_0 F_{0(0)}^2 - 2\lambda_0 F_{0(1)} . \quad (6.5)$$

7. Removing self-energy insertions ($a = 3$)



After having removed the tadpoles and the seagulls, we remove the self-energy insertions. The recursion relation becomes, in diagrams, Fig. 5. The equation for the case $a = 3$ becomes

$$F = z + g\left(F^3 - \frac{F-1}{z}\right) + \lambda\left(F^3 + \frac{2F^2}{z} + \frac{F-z-z^2F_{(2)}}{z^2}\right) - CF, \quad (7.1)$$

with

$$F_{(1)} = 1, \quad \text{or} \quad F = z + F_{(2)}z^2 + \mathcal{O}(z^3). \quad (7.2)$$

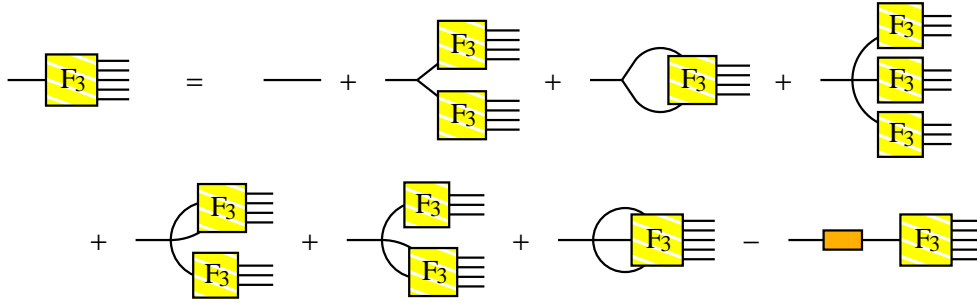


Figure 5. Removing self-energies.

In (7.1), the last term removes everything that might have produced a self-energy insertion up front. This includes the seagull contribution, which is therefore removed automatically, so that the corresponding term in Eq. (6.1), being $-2\lambda F F_{(1)}$, could be left out. It just readjusts the z -independent number C .

C is now fixed by the requirement (7.2), $F_{3(1)} = 1$. Comparing Eq. (7.1) with (5.3) gives us the relations

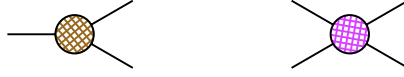
$$F_3 = Q_3 F_1; \quad z_3 = z_1/Q_3; \quad 1 + C = 1/Q_3^2; \quad (7.3)$$

$$g_3 = g_1/Q_3^3; \quad \lambda_3 = \lambda_1/Q_3^4; \quad (7.4)$$

$$Q_3^2 = 1/F_{1(1)}; \quad (Q_1 Q_3)^2 = 1/F_{0(1)}. \quad (7.5)$$

It is easy to see that these are merely field renormalizations that replace the dressed propagators by bare ones.

8. Removing dressed 3-vertices and dressed 4-vertices



The last two steps are remarkably easy. Recursion relations for the last two cases are not so easy to write down, but they are not needed. The amplitudes considered remain the same, but only the definitions of the coupling constants change. All one does is recombine all contributions from subgraphs that express dressed 3-point vertex insertions and use these to redefine the coupling constant g . After this, we do the same with the 4-vertex contributions to redefine λ . See Fig. 6.

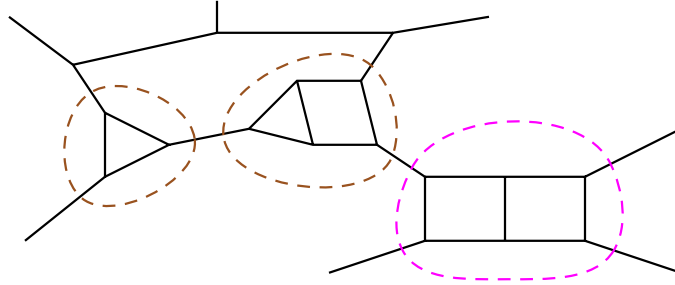


Figure 6. Collecting 3- and 4-point subgraphs.

This allows us to write:

$$F_4 = F_3 ; \quad z_4 = z_3 ; \quad (8.1)$$

$$g_4 = F_{3(2)} = Q_3^3 F_{1(2)} = (Q_1 Q_3)^3 F_{0(2)} = \frac{F_{0(2)}}{F_{0(1)}^{3/2}} . \quad (8.2)$$

$$\lambda_4 = \lambda_3 , \quad (8.3)$$

and when we also remove the dressed 4-vertices:

$$F_5 = F_3 ; \quad z_5 = z_3 ; \quad (8.4)$$

$$g_5 = g_4 = F_{0(2)}/F_{0(1)}^{3/2} ; \quad (8.5)$$

$$\begin{aligned} \lambda_5 = \Gamma_{3(1)} &= F_{3(3)} - 2 F_{3(2)}^2 = \frac{F_{1(1)} F_{1(3)} - 2 F_{1(2)}^2}{F_{1(1)}^3} \\ &= \frac{F_{0(1)} F_{0(3)} - 2 F_{0(2)}^2}{F_{0(1)}^3} . \end{aligned} \quad (8.6)$$

9. Critical couplings

At high orders, the number of diagrams can be read off from the values of g and λ where the amplitudes develop their first singularities. These occur when the elimination process of p and q in Eqs. (3.16)–(3.19) develops branch points. A branch point is a set of values for p and q where a small variation (dp, dq) produces a vanishing variation $(dg, d\lambda)$. Or,

$$\det \begin{vmatrix} \frac{\partial g}{\partial p} & \frac{\partial g}{\partial q} \\ \frac{\partial \lambda}{\partial p} & \frac{\partial \lambda}{\partial q} \end{vmatrix} = 0 . \quad (9.1)$$

The solution of this equation was found to be

$$\begin{aligned} p &= t\sqrt{z} ; \\ q &= z - 1 ; \quad z = \frac{12 - 4t^3 + t^4}{6 - 6t - 3t^2 + 2t^3} . \end{aligned} \quad (9.2)$$

At these points, we have $(g_a, \lambda_a) = (g_a^c, \lambda_a^c)$, with

$$g_0^c = \frac{\pm 2(3-t)t^2(6-6t-3t^2+2t^3)^{1/2}}{(12-4t^3+t^4)^{3/2}} ; \quad (9.3)$$

$$\lambda_0^c = \frac{(2+2t-t^2)(6-6t-3t^2+2t^3)}{(12-4t^3+t^4)^2} . \quad (9.4)$$

The most important region, where $g > 0$ and $\lambda > 0$, is from $t = 1 - \sqrt{3}$ (where $\lambda_0^c = 0$, $g_0^c = 1/\sqrt{12\sqrt{3}}$) to $t = 0$ (where $\lambda_0^c = 1/12$, $g_0^c = 0$).

An important non-trivial finding is that for the critical line near the origin, where Eq. (9.1) holds, one also has, for the functions α and β defined in Eq. (3.9),

$$\frac{\partial \alpha}{\partial p} / \frac{\partial \alpha}{\partial q} = \frac{\partial \beta}{\partial p} / \frac{\partial \beta}{\partial q} = \frac{\partial g}{\partial p} / \frac{\partial g}{\partial q} = \frac{\partial \lambda}{\partial p} / \frac{\partial \lambda}{\partial q} , \quad (9.5)$$

so that, at a critical point where $(dp, dq) \neq 0$, but $(dg, d\lambda) = 0$, one also has $(d\alpha, d\beta) = 0$, and since all other coupling parameters g_a, λ_a are built from α and β , we may conclude that the critical values of these other coupling constants directly follow from the critical values of the parameters p and q . In other words, Eqs. (9.2) apply to all critical couplings g_a, λ_a , $a = 0, \dots, 5$. Although this is what one would have expected on physical grounds (the divergence of the diagrams should not depend on the choice of coupling parameters), the mathematical reason for this phenomenon is not totally clear to the author.

The results for all critical lines are deferred to Appendix C. We depict the critical lines in Fig. 7. We see the regions of convergence grow as more constraints are imposed on the diagrams. The most surprising feature perhaps is the kinks in the curves at $g = 0$ (since diagrams assemble in even or odd functions of g , the picture is symmetric). One would have expected smooth, tilted lines if λ is plotted against g^2 , not g , so that the lines should run horizontally at $g = 0$ in the $g\lambda$ plane. But such is not the case. The complete courses in the (g^2, λ) plane of the critical curves at all t values is quite complex,

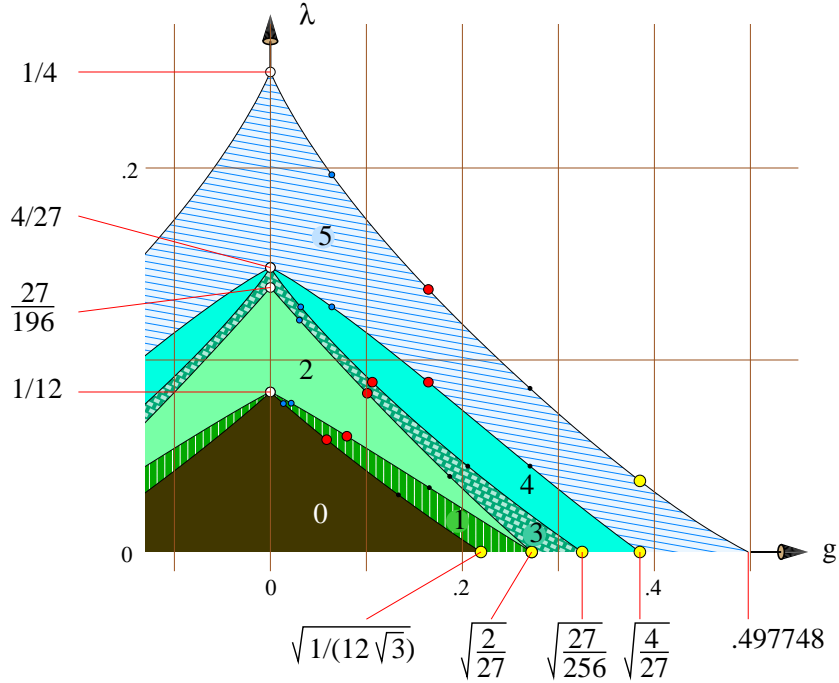


Figure 7. Convergence regions in the g, λ plane

The convergence domains for the cases $a = 0$ to 5 are shown. The picture is numerically accurate. Dots of equal colors and sizes correspond to equal values of p, q and t .

showing cusps, among others at $g^2 = 0$. In contrast, only the physical regions shown in Fig. 7 appear to be rather featureless. (the figure is highly accurate).

At zero g and at zero λ , the critical points are simple algebraic numbers, as indicated in Fig. 7; only at $\lambda_5^c = 0$, the value of g_5^c is a root of a polynomial of a high degree.

10. Conclusion

All interesting sets of planar diagrams can be counted, in the sense that the generating functions for their numbers can be found analytically. This provides us with exact descriptions of the critical lines in the g, λ plane. These lines show kinks at $g = 0$, where one would have expected analytic g^2 dependence. Fig. 7 shows the convergence regions accurately, when g and λ are positive and real. The detailed mathematical expressions are given in the appendices B and C.

References

1. G. 't Hooft, Nucl. Phys. **B72** (1974) 461; Nucl. Phys. **B75** (1974) 461.
2. H.B. Nielsen and P. Olesen, Phys. Letters **32 B** (1970)203;
B. Sakita and M.A. Virasoro, Phys. Rev. Letters **24** (1970) 1146;
H. Bohr and H.B. Nielsen, Nucl. Phys. **B227** (1983) 547.
3. J. Koplik, A. Neveu and S. Nussinov, Nucl. Phys. **B 123** (1977)109
4. W.T. Tutte, Can. J. Math. **14** (1962) 21.
5. E. Brézin, C. Itzykson, G. Parisi and J.B. Zuber, Commun. Math. Phys. **59** (1978) 35.
6. G. 't Hooft, Commun. Math. Phys. **88** (1983) 1; "Planar diagram field theories", in *Progress in Gauge Field Theory, NATO Adv. Study Inst. Series*, eds. G. 't Hooft et al., Plenum, 1984, p. 271.

Appendix A. Constructing perturbative planar QCD amplitudes at all orders without divergences

A renormalization scheme that appears to be not so well-known⁶ can be set up in the following way. It works particularly well for planar field theories in 4 space-time dimensions, but it also applies to several other quantum field theories, notably QED. Presumably, QCD with $N_c = 3$ can also be covered along these lines, but some technical details have not been worked out to my knowledge. This appendix gives a brief description.

Our scheme consists of first collecting all one-particle irreducible 2-, 3- and 4-point diagrams, and formally considering the non-local quartic effective action generated by these diagrams.

Next, consider all diagrams using the Feynman rules derived from this action, but *with the limitation that only those diagrams that are absolutely ultraviolet convergent are included*. No superficially ultraviolet divergent subgraph is accepted. To be precise, we omit all diagrams with 4 or less external lines, as well as all diagrams containing any non-trivial subdiagram with 4 or less external lines.

Clearly, one expects that the 1PI subgraphs with 4 or less external lines have already been taken care of by our use of the quartic effective action instead of the bare Lagrangian. The important issue to address is, whether the counting of all diagrams was done correctly so as to obtain the required physical amplitudes. But this is not difficult to prove:

Theorem: the above procedure correctly reproduces the complete amplitudes for the original theory. No diagrams are over-counted or under-counted.

The proof of the theorem is by inspection. Take any diagram of the original theory. Consider all its 2-, 3-, and 4-point subgraphs, and ascertain that these can be identified unambiguously as contributions of our effective Lagrangian. In practice, one draws circles around the subgraphs as illustrated in Fig. 6. Over- or under-counting can only happen if any ambiguity would arise with the identification. Such ambiguities can only be expected if

two subgraphs are connected by at least two lines. But if they both would have 4 external lines or less, the entire (sub-)diagram would have $4+4-2\times 2 = 4$ or less external lines, and this implies that this entire combination should itself be counted as one single contribution to the effective Lagrangian (see Fig. 8a).

If we would have tried to continue the procedure by including 5-point irreducible subgraphs into a quintic effective Lagrangian (or more), then counting problems would arise: $5 + 5 - 2 \times 2 > 5$ (see Fig. 8b)

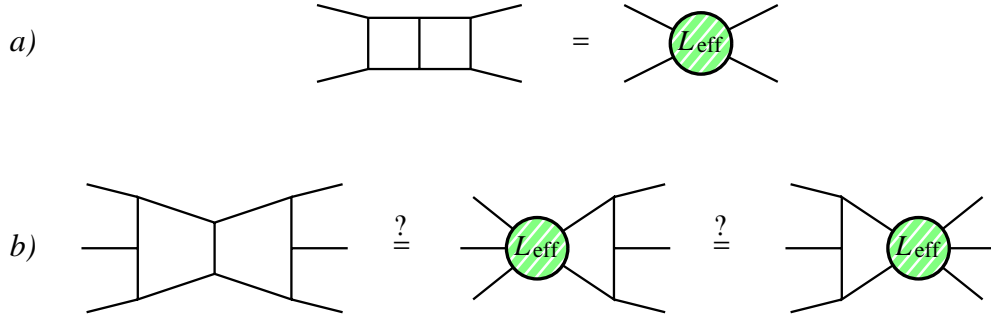


Figure 8. Ambiguity when including a 5-point vertex in the effective Lagrangian

From our theorem, one deduces that *if all one-particle irreducible 2-, 3-, and 4-point vertices are known, all amplitudes can be derived without encountering any divergent (sub-)graph(s).*

In a planar theory, the diagrams considered are of our class 5.

What remains to be done to complete a perturbative computational scheme, is to establish an algorithm to compute the irreducible 2-, 3-, and 4-point vertices (and, if they occur, the tadpole diagrams as well). Actually, this is simple. Consider a 4-point 1PI diagram $\Gamma(p_1, p_2, p_3, p_4)$. Here, p_μ are the external momenta, and $p_1 + p_2 + p_3 + p_4 = 0$. Now consider the difference

$$\Gamma(p_1 + k, p_2 - k, p_3, p_4) - \Gamma(p_1, p_2, p_3, p_4) \equiv k_\mu \Delta^\mu(p_1, \underline{k}, p_2 - k, p_3, p_4). \quad (A.1)$$

The underlining refers to the fact that, in the function Δ^μ , this external line follows distinct Feynman rules.

If we follow a path inside the diagram, we can consider the entire expression for Δ^μ as being built from expressions containing differences. For instance, in the propagators:

$$\frac{1}{(p+k)^2 + m^2} - \frac{1}{p^2 + m^2} = \frac{k_\mu (-2p - k)^\mu}{((p+k)^2 + m^2)(p^2 + m^2)}, \quad (A.2)$$

or else, in the 3-vertices:

$$(p+k)_\nu - p_\nu = k_\mu \delta^\mu_\nu. \quad (A.3)$$

We notice, that the expressions for Δ^μ are all (superficially) ultraviolet convergent! Actually, one may set up unambiguous Feynman rules for $\Delta^\mu(p_1, \underline{k}, p_2, -kp_3, p_4)$ and observe

that this amplitude exactly behaves as a 5-point diagram, hence it is (superficially) convergent.

For the 3-point and the 2-point diagrams, one can do exactly the same thing by differentiating more than once. In practice, what one finds is, that there is a set of rules containing fundamental irreducible 2-, 3- and 4-point vertices, and in addition rules to determine their differences at different values of their momenta. The complete procedure thus leads to the following situation.

We start by postulating the so-called ‘primary vertex functions’. These are, not only the irreducible 2-point functions[§] $\Gamma_{[2]}(p, -p)$, the irreducible 3-point functions $\Gamma_{[3]}(p_1, p_2, -p_1 - p_2)$ and the irreducible 4-point functions $\Gamma_{[4]}(p_1, \dots, p_4)$, but also, in addition, the difference functions $\Delta_{[2]}^\mu(p, \underline{k}, -p - k)$ and $\Delta_{[3]}^\mu(p_1, \underline{k}, p_2 - k, -p_1 - p_2)$, and finally the functions $U_{[2]}$, obtained by differentiating $\Delta_{[2]}^\mu$ once more:

$$\Delta_{[2]}^\mu(p_1 + q, p_2 - q, -p_1 - p_2) - \Delta_{[2]}^\mu(p_1, p_2, -p_1 - p_2) \equiv q_\nu U_{[2]}^{\mu\nu}(p_1 - q, \underline{\underline{q}}, p_2, -p_1 - p_2), \quad (A.4)$$

where one of the other external lines, p_1 or p_2 is underlined. The double underlining is here to denote that the two entries are to be treated distinctly (because of the factor k_μ , the functions $U_{[2]}^{\mu\nu}$ are not symmetric under interchange of k and q).

These primary vertex functions are derived by first considering the differences for $\Gamma_{[4]}$, $\Delta_{[3]}^\mu$ and $U_{[2]}^{\mu\nu}$ at two different sets of external momenta. These expressions are handled as if they were irreducible 5-point diagrams. These are expanded in terms of planar diagrams where all irreducible subgraphs of 4 or less external lines are bundled to form the primary vertex functions. At one of the the edges of such a diagram, we then encounter one of the functions Δ^μ or $U^{\mu\nu}$.

This way, we arrive at difference equations for the primary vertices, with at the r.h.s. again the primary vertices. The primary vertices $\Gamma_{[3]}$, $\Delta_{[2]}^\mu$ and $\Gamma_{[2]}$ are then obtained by integrating $\Delta_{[3]}^\mu$, $U_{[2]}^{\mu\nu}$ and $\Delta_{[2]}^\mu$ with respect to the external momenta. This completes the procedure to obtain all amplitudes by iteration.

Technical implementation of our scheme requires that in all diagrams, an unambiguous path can be defined from one external line to another. In QED, one may use the paths defined by the electron lines. In a planar theory, one may define the paths to run along the edges of a diagram.

Three remarks are of order:

1. The procedure is effectively a renormalization group procedure. The functions Δ^μ and $U^{\mu\nu}$ play the role of beta functions.
2. The procedure is essentially still perturbative, since the planar diagrams must still be summed. Our beta functions are free of ultraviolet divergences, but the summation over planar diagrams may well diverge.

[§] Here, the entries in the square brackets [...] differ from the ones in the curved brackets (...) of Sect. (4) by one unit.

3. The procedure only works if the integrations do not lead to clashes. This implies that it is not to be viewed as a substitute for regularization procedures such as dimensional regularization. We still need dimensional regularization if we want to *prove* that the method is unambiguous, which, of course, it is, in the case of planar QCD.

Appendix B. The power expansions in g and λ .

To illustrate how our expressions count diagrams, we produce the first few terms of the power expansions in g and λ .

The case $a = 0$.

Let us consider the double series expansions of g and λ with respect to p and q . Expanding Eqs. (3.16) and (3.17), we get

$$\begin{aligned}
g_0 = & \left(\frac{1}{2} - \frac{3}{2}q + \frac{5}{2}q^2 - \frac{7}{2}q^3 + \frac{9}{2}q^4 - \frac{11}{2}q^5 + \frac{13}{2}q^6 \right) p + \\
& \left(\frac{3}{4} - \frac{13}{6}q + \frac{17}{4}q^2 - 7q^3 + \frac{125}{12}q^4 - \frac{29}{2}q^5 + \frac{77}{4}q^6 \right) p^3 + \\
& \left(\frac{7}{24} - \frac{25}{24}q + \frac{29}{12}q^2 - \frac{55}{12}q^3 + \frac{185}{24}q^4 - \frac{287}{24}q^5 + \frac{35}{2}q^6 \right) p^5 + \mathcal{O}(p^7, q^7);
\end{aligned} \tag{B.1}$$

$$\begin{aligned}
\lambda_0 = & \frac{1}{3}q - \frac{2}{3}q^2 + q^3 - \frac{4}{3}q^4 + \frac{5}{3}q^5 - 2q^6 + \\
& \left(-\frac{1}{3} + q - 2q^2 + \frac{10}{3}q^3 - 5q^4 + 7q^5 - \frac{28}{3}q^6 \right) p^2 + \\
& \left(-\frac{1}{6} + \frac{11}{18}q - \frac{13}{9}q^2 + \frac{25}{9}q^3 - \frac{85}{18}q^4 + \frac{133}{18}q^5 - \frac{98}{9}q^6 \right) p^4 + \mathcal{O}(p^6, q^7).
\end{aligned} \tag{B.2}$$

Such expansions will be displayed in a short-hand notation:

$$g_0(p, q) = \begin{matrix} & 1 & q & q^2 & q^3 & q^4 & q^5 & q^6 \\ p & \left(\frac{1}{2} & -\frac{3}{2} & \frac{5}{2} & -\frac{7}{2} & \frac{9}{2} & -\frac{11}{2} & \frac{13}{2} \right) \\ p^3 & \left(\frac{3}{4} & -\frac{13}{6} & \frac{17}{4} & -7 & \frac{125}{12} & -\frac{29}{2} & \frac{77}{4} \right) \\ p^5 & \left(\frac{7}{24} & -\frac{25}{24} & \frac{29}{12} & -\frac{55}{12} & \frac{185}{24} & -\frac{287}{24} & \frac{35}{2} \right) \end{matrix} \tag{B.3}$$

$$\lambda_0(p, q) = \begin{matrix} & 0 & \frac{1}{3} & -\frac{2}{3} & 1 & -\frac{4}{3} & \frac{5}{3} & -2 \\ p^2 & \left(-\frac{1}{3} & 1 & -2 & \frac{10}{3} & -5 & 7 & -\frac{28}{3} \right) \\ p^4 & \left(-\frac{1}{6} & \frac{11}{18} & -\frac{13}{9} & \frac{25}{9} & -\frac{85}{18} & \frac{133}{18} & -\frac{98}{9} \right) \end{matrix} \tag{B.4}$$

Of course, the matrices extend to infinity. We invert the series^{||} in x and y :

$$p(g_0, \lambda_0) = \begin{matrix} & \lambda_0 & \lambda_0^2 & \lambda_0^3 & \lambda_0^4 & \lambda_0^5 \\ g_0 & \begin{pmatrix} 2 & 18 & 180 & 1890 & 20412 & 224532 \\ g_0^3 & \begin{pmatrix} 12 & 368 & 7860 & 143424 & 2393496 & 37700640 \\ g_0^5 & \begin{pmatrix} 128 & 7120 & 240768 & 6390720 & 146382336 & 3033374832 \end{pmatrix} \end{pmatrix} \end{pmatrix} \end{matrix} \quad (B.5)$$

$$q(g_0, \lambda_0) = \begin{matrix} g_0^2 & \begin{pmatrix} 0 & 3 & 18 & 135 & 1134 & 10206 \\ 4 & 84 & 1368 & 20196 & 283176 & 3847176 \\ g_0^4 & \begin{pmatrix} 40 & 1768 & 49656 & 1127808 & 22584528 & 415844280 \end{pmatrix} \end{pmatrix} \end{matrix} \quad (B.6)$$

The first Green functions are then

$$F_{0(0)}(g_0, \lambda_0) = \begin{matrix} g_0 & \begin{pmatrix} 1 & 6 & 45 & 378 & 3402 & 32076 \\ g_0^3 & \begin{pmatrix} 4 & 92 & 1572 & 23904 & 341928 & 4712580 \\ g_0^5 & \begin{pmatrix} 32 & 1424 & 40128 & 912960 & 18297792 & 337041648 \end{pmatrix} \end{pmatrix} \end{pmatrix} \end{matrix} \quad (B.7)$$

$$F_{0(1)}(g_0, \lambda_0) = \begin{matrix} g_0^2 & \begin{pmatrix} 1 & 2 & 9 & 54 & 378 & 2916 \\ 3 & 48 & 630 & 7776 & 93555 & 1111968 \\ g_0^4 & \begin{pmatrix} 24 & 856 & 20112 & 392040 & 6868152 & 112295160 \end{pmatrix} \end{pmatrix} \end{matrix} \quad (B.8)$$

The case $a = 1$.

From now on, we leave the powers of g and λ to be understood. Whether the g 's come in even or odd powers depends on whether the number of external lines is even or odd. Before looking at these numbers, we continue to produce more lists. From Eqs. (5.6) and (5.7):

$$g_1(p, q) = \begin{pmatrix} \frac{1}{2} & -1 & 1 & -1 & 1 & -1 \\ \frac{5}{8} & -\frac{95}{48} & \frac{109}{24} & -\frac{65}{8} & \frac{301}{24} & -\frac{427}{24} \\ \frac{149}{192} & -\frac{823}{192} & \frac{10453}{768} & -\frac{4183}{128} & \frac{25513}{384} & -\frac{46309}{384} \end{pmatrix} \quad (B.9)$$

$$\lambda_1(p, q) = \begin{pmatrix} 0 & \frac{1}{3} & -\frac{2}{3} & 1 & -\frac{4}{3} & \frac{5}{3} \\ -\frac{1}{3} & \frac{4}{3} & -\frac{23}{6} & \frac{26}{3} & -\frac{33}{2} & 28 \\ -\frac{1}{2} & \frac{127}{36} & -\frac{499}{36} & \frac{5765}{144} & -\frac{6883}{72} & \frac{28807}{144} \end{pmatrix} \quad (B.10)$$

^{||} For the inversion, a few more terms not shown in Eqs. (B.3–4) were needed. Similarly, Eqs. (B.11) and (B.12) required a few terms not shown in (B.9,10). The coefficients that we do show are the correct first few terms of the infinite series expansions.

Inverting this gives:

$$p(g_1, \lambda_1) = \begin{pmatrix} 2 & 12 & 108 & 1080 & 11340 & 122472 \\ 6 & 143 & 2700 & 45441 & 714528 & 10741086 \\ 35 & 1685 & \frac{201447}{4} & \frac{2425941}{2} & 25670925 & 497809800 \end{pmatrix} \quad (B.11)$$

$$q(g_1, \lambda_1) = \begin{pmatrix} 0 & 3 & 18 & 135 & 1134 & 10206 \\ 4 & 48 & 666 & 9072 & 120852 & 1582416 \\ 16 & 592 & 14328 & 292869 & 5416524 & 93623769 \end{pmatrix} \quad (B.12)$$

Now, $F_{1(0)} = 0$. The next Green functions are found by expanding Eq. (5.5), using (5.3) Or (3.2):

$$F_{1(1)}(g_1, \lambda_1) = \begin{pmatrix} 1 & 2 & 9 & 54 & 378 & 2916 \\ 1 & 15 & 189 & 2268 & 26730 & 312741 \\ 4 & 132 & 2925 & 54432 & 917973 & 14535288 \end{pmatrix} \quad (B.13)$$

$$F_{1(2)}(g_1, \lambda_1) = \begin{pmatrix} 1 & 9 & 81 & 756 & 7290 & 72171 \\ 4 & 99 & 1755 & 27216 & 393417 & 5450733 \\ 24 & 1044 & 28674 & 635607 & 12420216 & 223297074 \end{pmatrix} \quad (B.14)$$

The case $a = 2$. Similarly, we found:

$$F_{2(1)}(g_2, \lambda_2) = \begin{pmatrix} 1 & 0 & 1 & 2 & 10 & 42 \\ 1 & 5 & 35 & 228 & 1540 & 10439 \\ 4 & 60 & 725 & 7636 & 74725 & 695464 \end{pmatrix} \quad (B.15)$$

$$F_{2(2)}(g_2, \lambda_2) = \begin{pmatrix} 1 & 3 & 15 & 76 & 420 & 2409 \\ 4 & 45 & 435 & 3818 & 32025 & 260799 \\ 24 & 540 & 8370 & 107877 & 1245960 & 13365702 \end{pmatrix} \quad (B.16)$$

The case $a = 3$: $F_{3(1)} = 1$ and

$$F_{3(2)}(g_3, \lambda_3) = \begin{pmatrix} 1 & 3 & 12 & 55 & 273 & 1428 \\ 1 & 15 & 159 & 1460 & 12405 & 100449 \\ 3 & 90 & 1638 & 23400 & 288738 & 3227490 \end{pmatrix} \quad (B.17)$$

Concentrating now on the 1PI functions:

$$\Gamma_{3(3)}(g_3, \lambda_3) = \begin{pmatrix} 0 & 1 & 2 & 6 & 22 & 91 \\ 0 & 4 & 44 & 364 & 2720 & 19380 \\ 1 & 34 & 596 & 7852 & 88251 & 896972 \end{pmatrix} \quad (B.18)$$

$$\Gamma_{3(4)}(g_3, \lambda_3) = \begin{pmatrix} 0 & 0 & 5 & 45 & 315 & 2040 \\ 0 & 5 & 115 & 1565 & 16950 & 161950 \\ 1 & 65 & 1750 & 31890 & 465080 & 5873405 \end{pmatrix} \quad (B.19)$$

$$\Gamma_{3(5)}(g_3, \lambda_3) = \begin{pmatrix} 0 & 0 & 0 & 2 & 15 & 90 \\ 0 & 0 & 9 & 168 & 1938 & 18240 \\ 0 & 6 & 249 & 5176 & 77841 & 970596 \end{pmatrix} \quad (B.20)$$

$a = 4$: $\Gamma_{4(2)} = g_4$ and

$$\Gamma_{4(3)}(g_4, \lambda_4) = \begin{pmatrix} 0 & 1 & 2 & 6 & 22 & 91 \\ 0 & 4 & 20 & 112 & 660 & 4004 \\ 1 & 14 & 142 & 1288 & 10990 & 90174 \end{pmatrix} \quad (B.21)$$

$$\Gamma_{4(4)}(g_4, \lambda_4) = \begin{pmatrix} 0 & 0 & 5 & 30 & 165 & 910 \\ 0 & 5 & 65 & 560 & 4365 & 32585 \\ 1 & 35 & 550 & 6580 & 68740 & 661647 \end{pmatrix} \quad (B.22)$$

$$\Gamma_{4(5)}(g_4, \lambda_4) = \begin{pmatrix} 0 & 0 & 0 & 2 & 15 & 90 \\ 0 & 0 & 9 & 114 & 957 & 7098 \\ 0 & 6 & 159 & 2104 & 21909 & 203370 \end{pmatrix} \quad (B.23)$$

$a = 5$: $\Gamma_{5(3)} = \lambda_5$ and

$$\Gamma_{5(4)}(g_5, \lambda_5) = \begin{pmatrix} 0 & 0 & 5 & 10 & 25 & 70 \\ 0 & 5 & 15 & 70 & 355 & 1770 \\ 1 & 5 & 50 & 430 & 3240 & 22422 \end{pmatrix} \quad (B.24)$$

$$\Gamma_{5(5)}(g_5, \lambda_5) = \begin{pmatrix} 0 & 0 & 0 & 2 & 3 & 6 \\ 0 & 0 & 9 & 54 & 225 & 882 \\ 0 & 6 & 69 & 424 & 2535 & 14796 \end{pmatrix} \quad (B.25)$$

It is now illustrative to identify the diagrams that are being counted. We see that, in our formalism, the counting is efficient: each diagram is counted essentially just with the multiplicity factors of Fig. 1. The tadpole diagrams have at most a factor two if they differ from their mirror image. See Fig. 9.

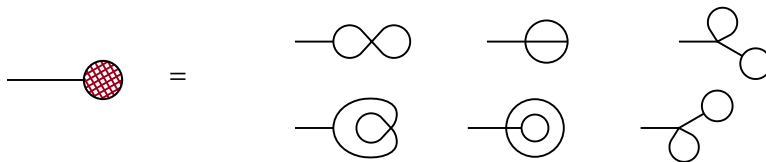


Figure 9. The six diagrams of $F_{0(0)}$ at order $g_0 \lambda_0$ (see Eq. (B.7)).

The two-point Green functions are separated in various classes by our scheme. In Fig. 10, we see the 48 diagrams of $F_{0(1)}$ at order $g^2 \lambda$, of which 15 belong to $F_{1(1)}$, and only 5 of those are in F_{21} (cf. Eqs. (B.8), (B.13) and (B.15)).

Similarly, we illustrate the contributions of different diagrams to the irreducible 5-point function, to order $g^5 \lambda$ (see Fig. 11). We see from Eqs. (B.19), (B.22) and (B.24) that $\Gamma_{3(4)}$ has 65 entries, $\Gamma_{4(4)}$ has 35, and $\Gamma_{5(4)}$ has only 5. The diagrams are shown in Fig. 11. Note that the distinction is whether there are non-trivial irreducible 3-point subgraphs present, or irreducible 4-point subgraphs.

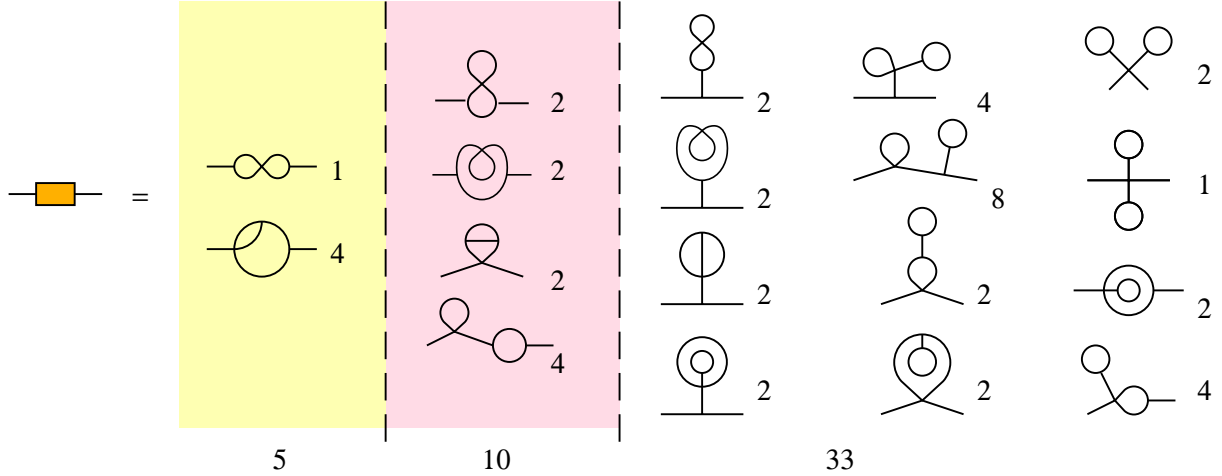


Figure 10. The 48 diagrams contributing to the 2 point function, at order $g^2\lambda$. 15 of these have no tadpole insertion; and 5 have also no seagull insertion.

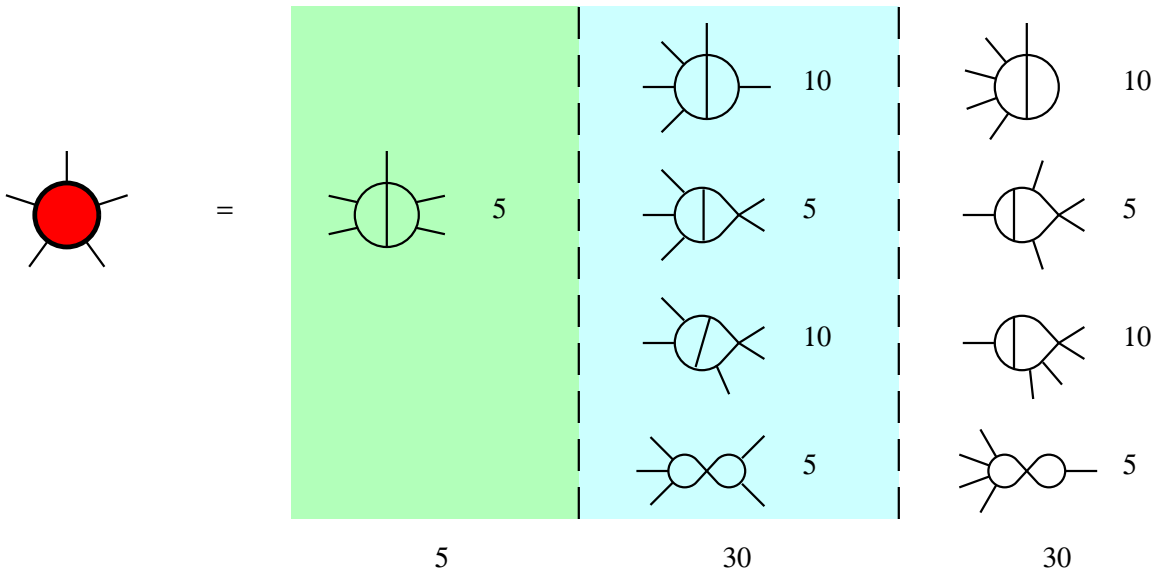


Figure 11. The 64 diagrams of $\Gamma_{3(4)}$, at order $g^5\lambda$, of which 35 are in $\Gamma_{4(4)}$ and 5 in $\Gamma_{5(4)}$.

Appendix C. The critical lines.

The critical lines (Fig. 7) are found by substituting Eqs. (9.2) in all our expressions. Here we give the outcomes. Starting from Eqs. (3.16)–(3.21), one just plugs in the equations (5.7), (5.9), (6.4), (6.5), (7.4), (7.5), (8.3) and (8.6), and uses the values of $F_{0(i)}$ as they follow from Eq. (3.2). We ignore the minus sign in (9.3), which is trivial. The results are the following algebraic expressions.

$$g_0^c = 2t^2(3-t)(6-6t-3t^2+2t^3)^{1/2}(12-4t^3+t^4)^{-3/2}; \quad (C.1)$$

$$\lambda_0^c = (2 + 2t - t^2)(6 - 6t - 3t^2 + 2t^3)(12 - 4t^3 + t^4)^{-2}. \quad (C.2)$$

$$g_1^c = \frac{2t^2(6 - t^2)^2(6 - 6t - 3t^2 + 2t^3)^{5/2}}{3^{3/2}(144 - 288t + 192t^3 - 168t^4 - 48t^5 + 100t^6 - 8t^7 - 17t^8 + 4t^9)^{3/2}}; \quad (C.3)$$

$$\lambda_1^c = \frac{(2 + 2t - t^2)(6 - 6t - 3t^2 + 2t^3)^5}{9(144 - 288t + 192t^3 - 168t^4 - 48t^5 + 100t^6 - 8t^7 - 17t^8 + 4t^9)^2}. \quad (C.4)$$

$$g_2^c = \frac{2t^2(6 - t^2)^2(6 - 6t - 3t^2 + 2t^3)^{5/2}}{(336 - 672t + 384t^2 + 256t^3 - 712t^4 + 48t^5 + 308t^6 - 56t^7 - 45t^8 + 12t^9)^{3/2}}; \quad (C.5)$$

$$\lambda_2^c = \frac{(2 + 2t - t^2)(6 - 6t - 3t^2 + 2t^3)^5}{(336 - 672t + 384t^2 + 256t^3 - 712t^4 + 48t^5 + 308t^6 - 56t^7 - 45t^8 + 12t^9)^2}. \quad (C.6)$$

$$g_3^c = \frac{2t^2(6 - t^2)^2(24 - 72t - 12t^2 + 56t^3 - 10t^4 - 10t^5 + 3t^6)^{3/2}}{(6 - 6t - 3t^2 + 2t^3)^5}; \quad (C.7)$$

$$\lambda_3^c = \frac{(2 + 2t - t^2)(24 - 72t - 12t^2 + 56t^3 - 10t^4 - 10t^5 + 3t^6)^2}{(6 - 6t - 3t^2 + 2t^3)^5}. \quad (C.8)$$

$$g_4^c = \frac{2t^2(6 - t^2)^2(6 - 3t^2 + t^3)}{(24 - 72t - 12t^2 + 56t^3 - 10t^4 - 10t^5 + 3t^6)^{3/2}}; \quad (C.9)$$

$$\lambda_4^c = \lambda_3^c. \quad (C.10)$$

$$g_5^c = g_4^c; \quad (C.11)$$

$$\begin{aligned} \lambda_5^c = & (3456 - 31104t + 25920t^2 + 55296t^3 - 180576t^4 - 44064t^5 + \\ & + 247824t^6 - 27936t^7 - 147672t^8 + 52760t^9 + 38076t^{10} - 24432t^{11} - \\ & - 1762t^{12} + 4506t^{13} - 921t^{14} - 202t^{15} + 114t^{16} - 18t^{17} + t^{18}) \times \\ & (24 - 72t - 12t^2 + 56t^3 - 10t^4 - 10t^5 + 3t^6)^{-3}. \end{aligned} \quad (C.12)$$

The curves of Fig. 7 are obtained by plotting λ_a^c against g_a^c , using t as a parameter.

In all plots, t runs from $1 - \sqrt{3}$ to 0, except for $a = 5$, where t runs from $-.890145$ to 0. The new lower bound is the closest zero of Eq. (C.12) for λ_5^c . The physical reason why this larger domain is needed is easy to understand: removing the irreducible 4-point diagrams that only contain 3-point vertices can only happen by invoking a negative counter term in λ .